

Unsteady MHD-Free Convection Flow Past from a Rotating Vertical Plate with the Influence of Hall and Ion-slip Current

M. Wahiduzzaman¹, Gopal Chandra Mazumder², Md. Tajul Islam³, A. Sarker⁴ and M.S. Uddin⁵

^{1,4,5}Mathematics Discipline, Khulna University, Khulna-9208, Bangladesh

²Upazilla Secondary Education Officer, Directorate of Secondary and Higher Education Ministry of Education, Chougacha, Jessore, Bangladesh

³ Department of Mathematics, Begum Rokeya University, Rangpur, Bangladesh

¹Corresponding author's email: wahidmathku@gmail.com

Received 12 December 2014; accepted 5 January 2015

Abstract. Viscous dissipation and Joule heating effects on unsteady MHD combined heat and mass transfer flow through hall and ion-slip currents along a semi-infinite vertical plate in a rotating system has been studied numerically. The boundary layer equations have been transformed into dimensionless coupled nonlinear ordinary differential equations by using appropriate transformations. The similarity solutions of the transformed dimensionless equations for the flow field and heat and mass transfer characteristics are obtained by explicit finite difference method. Numerical results are presented in the form of primary and secondary velocities, and temperature for different parameters entering into the analysis. Finally, the effects of the pertinent parameters on the Skin-friction coefficients and Nusselt number are also examined.

Keywords: MHD, Joule heating, Hall current, Ion-Slip current and rotating system

AMS Mathematics Subject Classification (2010): 76A25

1. Introduction

Coriolis force is very significant in a rotating system, the as compared to viscous and inertia forces occurring in the basic fluid equations. Considering this aspect of the rotational flows, model studies were carried out on MHD free convection and mass transfer flows in a rotating system by many investigators of whom the names Debnath (1975), Debnath et al. [1], Raptis and Perdakis [2] are worth mentioning. The influence of a transverse uniform magnetic field on the flow of a conducting fluid between two infinite parallel, stationary, and insulated plates has been studied by Hartmann and Lazarus [3]. A lot of research works concerning the Hartmann flow have been obtained under different physical effects. In most cases the Hall and Ion-slip terms were ignored in applying Ohm's law as they have no mentionable effect for small and moderate values of the magnetic field. Sattar and Alam [4] presented unsteady free convection and mass

M. Wahiduzzaman, G.C.Mazumder, Md. Tajul Islam, A.Sarker and M.S.Uddin

transfer flow of a viscous, incompressible and electrically conduction fluid past a moving infinite vertical porous plate with thermal diffusion effect. Saidul Islam et. al. [5] investigate the MHD Free Convection and Mass Transfer Flow with Heat Generation through an Inclined Plate. Abdur Rahman et al. [6] studied the thermophoresis Effect on MHD Forced Convection on a Fluid over a Continuous Linear Stretching Sheet in Presence of Heat Generation and Power-Law Wall Temperature. Hasanuzzaman et al. studied the ofsimilarity solution of unsteady combined free and force convective laminar boundary layer flow about a vertical porous surface with suction and blowing. Abo-Eldahab and El Aziz [7] have studied viscous dissipation and joule heating effects on MHD-free convection from a vertical plate with power-law variation in surface temperature in the presence of Hall and ion-slip currents. Present study investigate the work of El Aziz [5] for rotation case.

2. Governing equation

Consider a unsteady, laminar, free convection flow along a vertical semi-infinite rotating plate with the origin at the leading edge. Introducing Cartesian coordinate system, the x - axis is chosen along the plate in the direction of the flow and the y -axis is normal to it and the z axis be coincident with the leading edge. An external strong magnetic is applied in the y -direction and has a constant flux density \mathbf{B}_0 (see Figure 1). The effect of Hall and Ion-slip current gives rise to a force in the z -direction, which induces across flow in that direction, and hence the flow becomes three-dimensional. To simplify the analysis, we assume that there is no variation of flow and heat transfer quantities in the z -direction. Initially we consider that the plate as well as the fluid is at the same temperature. Also it is assumed that the fluid and the plate is at rest after that the plate is to be moving with a constant velocity. U_0 in its own plane and instantaneously at time $t > 0$, the temperature of the plate raised to $T_w (> T_\infty)$ which is there after maintained constant, where T_w is temperature at the wall and T_∞ is the temperature of the species far away from the plate. Under the usual boundary layer and Boussinesq approximation, the governing equation in (x, y, z) -coordinate for the problem under consideration can be written as follows:

Within the framework of the above stated assumptions with reference to the generalized equations, the equations relevant to the transient two dimensional problems are governed by the following system of coupled non-linear partial differential equations.

The continuity equation;
$$\frac{\partial u}{\partial x} + \frac{\partial v}{\partial y} = 0 \quad (1)$$

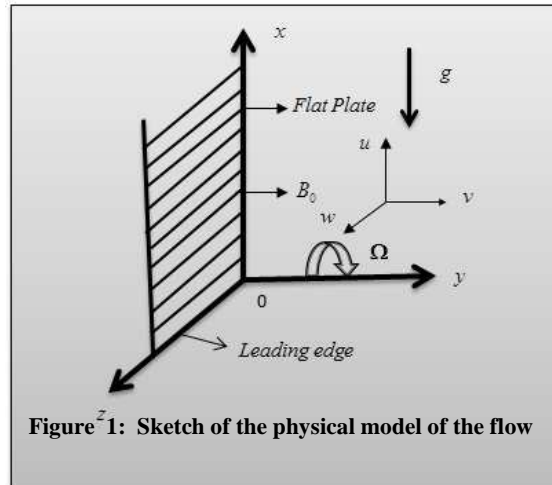


Figure 1: Sketch of the physical model of the flow

Unsteady MHD-Free Convection Flow Past from a Rotating Vertical Plate

Momentum equation in x -direction;

$$\frac{\partial u}{\partial t} + u \frac{\partial u}{\partial x} + v \frac{\partial u}{\partial y} = \nu \left(\frac{\partial^2 u}{\partial y^2} \right) + g\beta(T - T_\infty) + 2w\Omega - \frac{B^2 \sigma_e}{\rho(\alpha_e^2 + \beta_e^2)} [\alpha_e u + \beta_e w] \quad (2)$$

Momentum equation in z -direction;

$$\frac{\partial w}{\partial t} + u \frac{\partial w}{\partial x} + v \frac{\partial w}{\partial y} = \nu \left(\frac{\partial^2 w}{\partial y^2} \right) - 2u\Omega + \frac{B^2 \sigma_e}{\rho(\alpha_e^2 + \beta_e^2)} [\beta_e u - \alpha_e w] \quad (3)$$

Energy equation;

$$\frac{\partial T}{\partial t} + u \frac{\partial T}{\partial x} + v \frac{\partial T}{\partial y} = \frac{k}{\rho C_p} \left(\frac{\partial^2 T}{\partial y^2} \right) + \frac{Q}{\rho C_p} (T - T_\infty) + \frac{\mu}{\rho C_p} \left[\left(\frac{\partial u}{\partial y} \right)^2 + \left(\frac{\partial w}{\partial y} \right)^2 \right] + \frac{\sigma_e B_0^2}{\rho C_p (\alpha_e^2 + \beta_e^2)} (u^2 + w^2) \quad (4)$$

With the corresponding initial and boundary conditions are

$$t \leq 0, \quad u \rightarrow 0, w \rightarrow 0, T \rightarrow T_\infty \quad \text{at } x=0, y > 0 \quad (5)$$

$$t > 0 \quad u = 0, v = 0, w = 0, T = T_w \quad \text{at } y=0, x > 0$$

$$u \rightarrow 0, w \rightarrow 0, T \rightarrow T_\infty \quad \text{at } y \rightarrow \infty \quad (6)$$

where (u, v, w) are the velocity components along the (x, y, z) axes, respectively, T be the fluid temperature, σ_e is the electrical conductivity, e is the electron charge. ρ, ν and C_p are the density, kinematic viscosity and specific heat at constant pressure of the fluid, respectively. β, Q, g and k are the coefficient of thermal expansion, volumetric rate of heat generation, acceleration due to gravity and thermal conductivity, respectively, $\alpha_e = 1 + \beta_i \beta_e$, β_e and β_i are Hall and Ion-slip currents.

3. Mathematical formulation

Introducing the following dimensionless variables to the governing equations (1)-(4) and initial (5) and boundary (6) conditions;

$$X = \frac{xU_0}{\nu}, Y = \frac{yU_0}{\nu}, U = \frac{u}{U_0}, V = \frac{v}{U_0}, \tau = \frac{tU_0^2}{\nu}, \bar{T} = \frac{T - T_\infty}{T_w - T_\infty}$$

From the above dimensionless variable we have

$$u = U_0 U, v = U_0 V, T = T_\infty + (T_w - T_\infty) \bar{T}$$

Using these relations we have the following derivatives

$$\begin{aligned} \frac{\partial u}{\partial t} &= \frac{U_0^3}{\nu} \frac{\partial U}{\partial \tau}, \quad \frac{\partial u}{\partial x} = \frac{U_0^2}{\nu} \frac{\partial U}{\partial X}, \quad \frac{\partial u}{\partial y} = \frac{U_0^2}{\nu} \frac{\partial U}{\partial Y}, \quad \frac{\partial^2 u}{\partial y^2} = \frac{U_0^3}{\nu^2} \frac{\partial^2 U}{\partial Y^2}, \\ \frac{\partial w}{\partial t} &= \frac{U_0^3}{\nu} \frac{\partial W}{\partial \tau}, \quad \frac{\partial w}{\partial x} = \frac{U_0^2}{\nu} \frac{\partial W}{\partial X}, \quad \frac{\partial w}{\partial y} = \frac{U_0^2}{\nu} \frac{\partial W}{\partial Y}, \quad \frac{\partial^2 w}{\partial y^2} = \frac{U_0^3}{\nu^2} \frac{\partial^2 W}{\partial Y^2}, \\ \frac{\partial T}{\partial t} &= \frac{U_0^2 (T_w - T_\infty)}{\nu} \frac{\partial \bar{T}}{\partial \tau}, \quad \frac{\partial T}{\partial x} = \frac{U_0 (T_w - T_\infty)}{\nu} \frac{\partial \bar{T}}{\partial X}, \quad \frac{\partial T}{\partial y} = \frac{U_0 (T_w - T_\infty)}{\nu} \frac{\partial \bar{T}}{\partial Y}, \end{aligned}$$

M. Wahiduzzaman, G.C.Mazumder, Md. Tajul Islam, A.Sarker and M.S.Uddin

$$\frac{\partial^2 T}{\partial y^2} = \frac{U_0^2 (T_w - T_\infty)}{v^2} \frac{\partial^2 \bar{T}}{\partial Y^2}$$

Now we substitute the values of the above derivatives into the equations (1)-(4) and after simplification we obtain the following nonlinear coupled partial differential equations in terms of dimensionless variables

$$\frac{\partial U}{\partial X} + \frac{\partial V}{\partial Y} = 0 \quad (7)$$

$$\frac{\partial U}{\partial \tau} + U \frac{\partial U}{\partial X} + V \frac{\partial U}{\partial Y} = \frac{\partial^2 U}{\partial Y^2} + G_r \bar{T} + 2E_k W - \frac{M}{\alpha_e^2 + \beta_e^2} (\alpha_e U + \beta_e W) \quad (8)$$

$$\frac{\partial W}{\partial \tau} + U \frac{\partial W}{\partial X} + V \frac{\partial W}{\partial Y} = \frac{\partial^2 W}{\partial Y^2} - 2E_k U + \frac{M}{\alpha_e^2 + \beta_e^2} (\beta_e U - \alpha_e W) \quad (9)$$

$$\frac{\partial \bar{T}}{\partial \tau} + U \frac{\partial \bar{T}}{\partial X} + V \frac{\partial \bar{T}}{\partial Y} = \frac{1}{P_r} \frac{\partial^2 \bar{T}}{\partial Y^2} + \gamma \bar{T} + E_c \left[\left(\frac{\partial U}{\partial X} \right)^2 + \left(\frac{\partial W}{\partial Y} \right)^2 \right] + \frac{ME_c}{\alpha_e^2 + \beta_e^2} (U^2 + W^2) \quad (10)$$

where, Prandtl number, $P_r = \frac{\nu \rho C_p}{k}$, Eckert number, $E_c = \frac{U_0^2}{C_p (T_w - T_\infty)}$, Grash of

number, $G_r = \frac{g \beta (T_w - T_\infty) \nu}{U_0^3}$, Heat Absorption coefficient, $\gamma = \frac{Q}{\rho C_p} \frac{\nu}{U_0^2}$, Magnetic

parameter, $M = \frac{B_0^2 \sigma_e \nu}{\rho U_0^2}$ Rotational parameter, $E_k = \frac{\Omega \nu}{U_0^2}$.

Also the associated initial and boundary conditions become

$$\tau \leq 0, \quad U = 0, W = 0, \bar{T} = 0, \quad \text{everywhere} \quad (11)$$

$$\tau > 0, \quad U = 0, V = 0, W = 0, \bar{T} = 1, \quad \text{at } Y = 0 \quad (12) \quad U = 0, V = 0, \bar{T} = 0, \quad \text{at } Y \rightarrow \infty$$

4. Numerical technique

A system of non-linear coupled partial differential equations with the boundary conditions is very difficult to solve numerically. Many physical phenomena in applied science and engineering when formulated into mathematical models fall into a category of systems known as non-linear coupled partial differential equations. Most of these problems can be formulated as second order partial differences equations. For obtaining the solution of such problems advanced numerical methods has been performed. The governing equations of our problem contain a system of partial differential equations which is transformed by usual transformation into a non-dimensional system of non-linear coupled partial differential equations with initial and boundary conditions. Hence the solution of our problem would be based on advanced numerical methods. The Explicit **Finite Difference Method** will be used for solving our obtained non-similar coupled partial differential equations.

5. Results and discussion

For the purpose of discussing the results of the problem, the approximate solutions are obtained for various parameters. In order to analyze the physical significance of the model, the steady state numerical values of the non-dimensional primary velocity U , secondary velocity W and temperature T within the boundary layer for different values of Magnetic parameter (M), Prandlt number (P_r), Ekman number (E_k), Heat absorption coefficient (γ), Hall parameter (β_e), Ion-slip parameter (β_i), Grashof number (G_r) and Eckert number (E_c) respectively has been computed. For the steady state solutions of the problem, the computations have been carried out up to $\tau = 80$. It is observed that the values of this computation, however, show little changes after $\tau = 30$. Thus the solution at $\tau = 30$ are essentially steady-state solutions. Since the most important fluids are atmospheric air, salt water and water, so the results are limited to $P_r = 0.72$ (Prandlt number for air at $20^\circ C$), $P_r = 1.0$ (Prandlt number for salt water at $20^\circ C$) and $P_r = 5.0$ (Prandlt number for water at $20^\circ C$). However the values of another parameter M , R , γ , β_e , β_i , E_c are chosen arbitrarily as $M = 0.3, 0.5, 0.7$, $R = 0.03, 0.05, 0.07$, $\gamma = 0.0, 0.01, 0.03$, $\beta_e = 0.06, 0.07, 0.09$, $\beta_i = 0.04, 0.06, 0.08$ and $E_c = 0.01, 0.02, 0.03$. Along with the obtained steady states solutions, the flow behavior in case of cooling problems has been discussed graphically. The profiles of primary velocity, secondary velocity and temperature distributions versus co-ordinate variable Y has been illustrated in Figs. 2-19. For the change of magnetic parameter (M), the primary, secondary velocity and temperature distributions have been illustrated in **Figs 2-4**. From these figures it has been observed that the primary velocity decreases as the increasing values of the magnetic parameter and the Secondary velocity increases with the increase of magnetic parameter and there are minor effects in temperature distribution. For the change of Eckert number (E_c), the primary, secondary velocity and temperature distributions have been illustrated in **Figs 5-7**. From these figures it has been observed that there are minor effects but increasing in the primary, secondary velocity and the temperature distribution with the increases of Eckert number. For the change of Ekman number (E_k), the primary, secondary velocity and temperature distributions have been illustrated in **Figs 8-10**. From these figures it has been observed that the primary velocity and secondary velocity decreases as the increasing values of the magnetic parameter and the Secondary velocity increases with the increase of Ekman number and there are also increasing effects in temperature distribution. For the change of Heat absorption parameter (γ), the primary, secondary velocity and temperature distributions have been illustrated in **Figs 11-13**. From this figures it has been seen that the primary velocity and temperature distribution increases as the increasing values of Heat absorption parameter. There is a minor effect in secondary velocity with the increasing values of Heat absorption parameter. For the change of Grashof number (G_r), the primary, secondary velocity and temperature distributions have been illustrated in **Figs**

M. Wahiduzzaman, G.C.Mazumder, Md. Tajul Islam, A.Sarker and M.S.Uddin

14-16. From this figures it has been seen that the primary velocity and temperature distribution decreases as the increasing values of Grashof number while secondary velocity is increasing with the increasing values of Heat Grashof number. For the change of Prandlt number (P_r), the primary, secondary velocity and temperature distributions have been illustrated in **Figs 17-19** from these figures it has been observed that the primary velocity and temperature are decreased as the increasing values of the Prandlt number and the Secondary velocity increases with the increase of Prandlt number. Now we discuss the behavior of the quantities of the chief physical interest as local Shear Stress (τ_{xL}) in x -direction, local Shear Stress (τ_{zL}) in z -direction and local Nusselt number (N_{uL}) and sequentially average shear stress (τ_{xA}) in x -direction, average shear stress (τ_{zA}) in z -direction and average Nusselt number (N_{uA}) for different values of Magnetic parameter (M), Prandlt number (P_r), Ekman number (E_k), Heat absorption coefficient (γ), Hall parameter (β_e), Ion-slip parameter (β_i), Grashof number (G_r) and Eckert number (E_c) respectively. For this purpose the numerical solutions of the above mentioned parameter have been computed and discussed graphically in **Figure 20-37**. The steady state local Shear Stress (τ_{xL}) in x -direction, local Shear Stress (τ_{zL}) in z -direction and local Nusselt Number (N_{uL}) verses Co-ordinate Variable, X are illustrated in **Figure 20-37**. **In Figure 20-22**, Steady-state local Shear Stress (τ_{xL}) in x -direction, local Shear Stress (τ_{zL}) in z -direction and local Nusselt number (N_{uL}) are plotted for different values of Magnetic parameter (M) where $P_r = 0.72$, $G_r = 2.0$, $E_c = 0.01$, $E_k = 0.03$, $\beta_i = 0.04$, $\beta_e = 0.06$ and $\gamma = 0.01$. It has found that Steady-state local Shear Stress (τ_{xL}) in x -direction and local Shear Stress (τ_{zL}) in z -direction decrease for increasing of Magnetic parameter (M) but there is minor effect on local Nusselt number (N_{uL}) for increasing of Magnetic parameter (M). **In Figure 23-25**, Steady-state local Shear Stress (τ_{xL}) in x -direction, local Shear Stress (τ_{zL}) in z -direction and local Nusselt number (N_{uL}) are plotted for different values of Eckert number (E_c) where $P_r = 0.72$, $G_r = 2.0$, $M = 0.05$, $E_k = 0.03$, $\beta_i = 0.04$, $\beta_e = 0.06$ and $\gamma = 0.01$. It has found that Steady-state local Shear Stress (τ_{xL}) in x -direction and local Shear Stress (τ_{zL}) in z -direction and local Nusselt number (N_{uL}) increase for increasing of Eckert number (E_c). **In Figure 26-28**, Steady-state local Shear Stress (τ_{xL}) in x -direction, local Shear Stress (τ_{zL}) in z -direction and local Nusselt number (N_{uL}) are plotted for different values of Ekman number (E_k), where $P_r = 0.72$, $G_r = 2.0$, $E_c = 0.01$, $M = 0.05$, $\beta_i = 0.04$, $\beta_e = 0.06$ and $\gamma = 0.01$. It

Unsteady MHD-Free Convection Flow Past from a Rotating Vertical Plate

has found that Steady-state local Shear Stress (τ_{xL}) in x – direction and local Shear Stress (τ_{zL}) in z – direction decrease for increasing of Ekman number (E_k), but there is minor effect on local Nusselt number (N_{uL}) for increasing of Ekman number (E_k). **In Figure 29-31**, Steady-state average Shear Stress (τ_{xA}) in x – direction, average Shear Stress (τ_{AL}) in z – direction and average Nusselt number (N_{uA}) are plotted for different values of Heat absorption coefficient (γ) where $P_r = 0.72$, $G_r = 2.0$, $E_c = 0.01$, $M = 0.05$, $\beta_e = 0.06$, $E_k = 0.03$, and $\beta_i = 0.04$. It has found that Steady-state average Shear Stress (τ_{xA}) in x – direction, average Shear Stress (τ_{AL}) in z – direction and average Nusselt number (N_{uA}) increase for increasing of Heat absorption coefficient (γ). **In Figure 32-34**, Steady-state average Shear Stress (τ_{xA}) in x – direction, average Shear Stress (τ_{AL}) in z – direction and average Nusselt number (N_{uA}) are plotted for different values of Grashof number (G_r) where $P_r = 0.72$, $\gamma = 0.01$, $E_c = 0.01$, $M = 0.05$, $\beta_e = 0.06$, $E_k = 0.03$, and $\beta_i = 0.04$. It has found that Steady-state average Shear Stress (τ_{xA}) in x – direction, average Shear Stress (τ_{AL}) in z – direction and average Nusselt number (N_{uA}) increase for increasing of Grashof number (G_r). **In Figure 35-37**, Steady-state average Shear Stress (τ_{xA}) in x – direction, average Shear Stress (τ_{AL}) in z – direction and average Nusselt number (N_{uA}) are plotted for different values of Prandlt number (P_r) where $P_r = 0.72$, $\gamma = 0.01$, $E_c = 0.01$, $M = 0.05$, $\beta_e = 0.06$, $E_k = 0.03$, and $\beta_i = 0.04$.

It has found that Steady-state average Shear Stress (τ_{xA}) in x – direction, average Shear Stress (τ_{AL}) in z – direction and average Nusselt number (N_{uA}) decrease for increasing of Prandlt number (P_r). The steady state Average Shear Stress (τ_{xA}) in x – direction, Average Shear Stress (τ_{AL}) in z – direction and Average Nusselt Number (N_{uA}) versus Co-ordinate Variable, X are illustrated in **Figure 38-49**. **In Figure 38-40**, Steady-state average Shear Stress (τ_{xA}) in x – direction, average Shear Stress (τ_{AL}) in z – direction and average Nusselt number (N_{uA}) are plotted for different values of Magnetic parameter (M) where $P_r = 0.72$, $G_r = 2.0$, $E_c = 0.01$, $E_k = 0.03$, $\beta_i = 0.04$, $\beta_e = 0.06$ and $\gamma = 0.01$.

It has found that the average Shear Stress (τ_{xA}) in x – direction, average Shear Stress (τ_{AL}) in z – direction and average Nusselt number (N_{uA}) decrease for increasing of Magnetic parameter (M). **In Figure 41-43**, Steady-state average Shear Stress (τ_{xA})

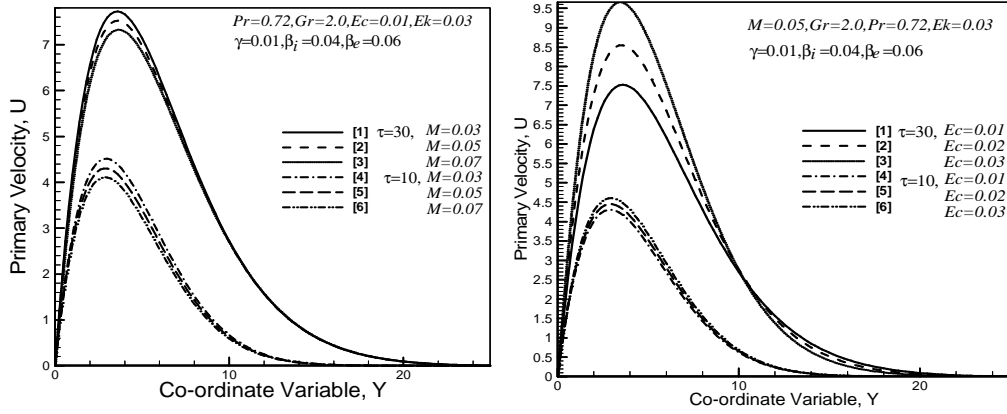


Figure 2: Primary velocity profiles for M . Figure 5: Primary velocity profiles for Ec

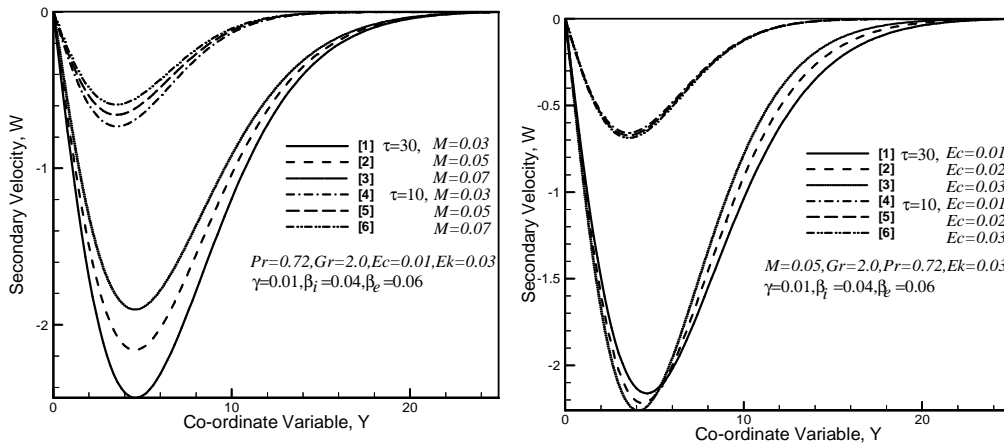


Figure 3: Secondary velocity for M .

Figure 6: Secondary velocity for Ec .

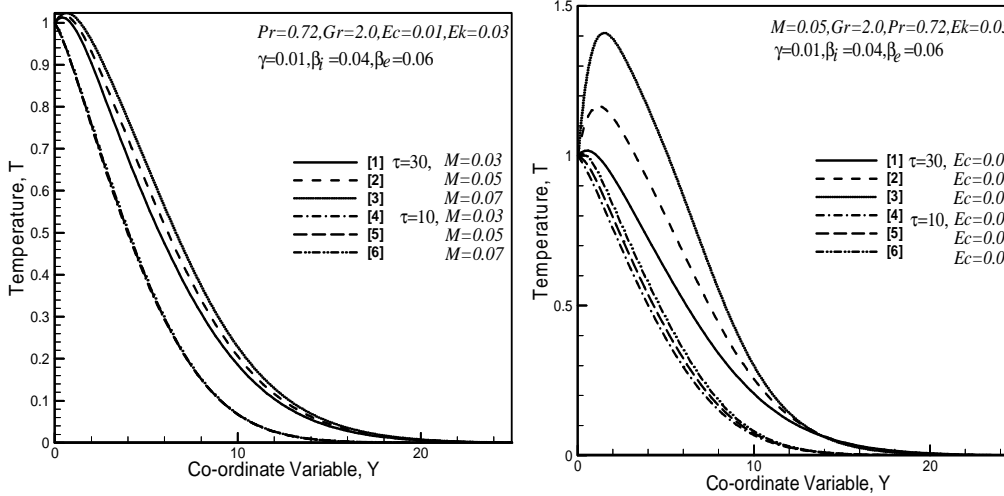


Figure 4: Temperature profiles for M

Figure 7: Temperature profiles for Ec

Unsteady MHD-Free Convection Flow Past from a Rotating Vertical Plate

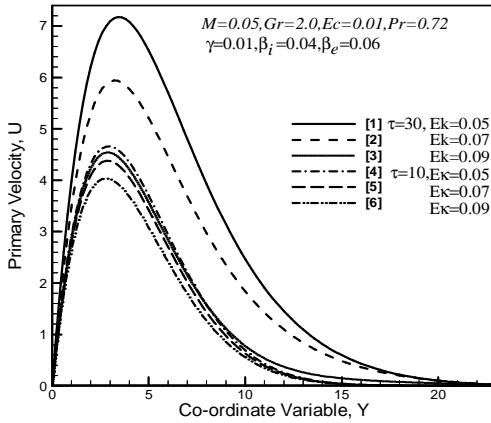


Figure 8: Primary velocity profiles for E_k

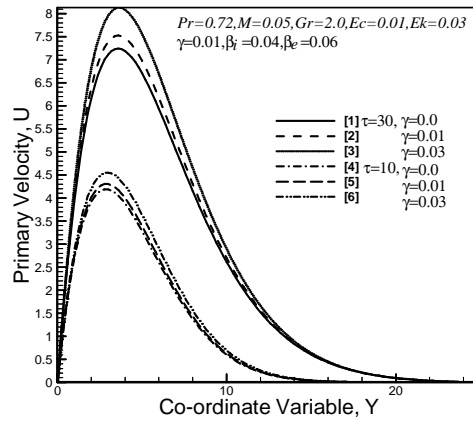


Figure 11: Primary velocity profiles for γ

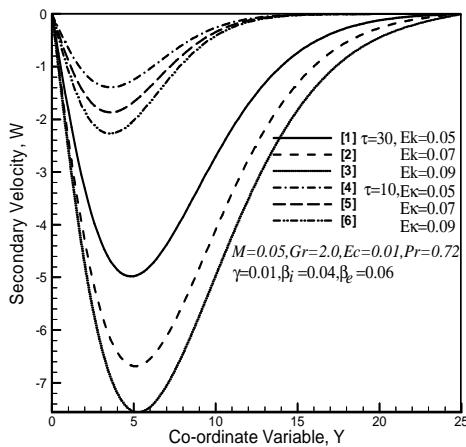


Figure 9: Secondary velocity for E_k

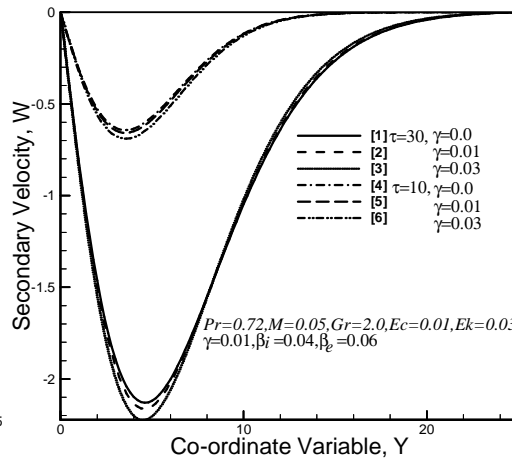


Figure 12: Secondary velocity for γ

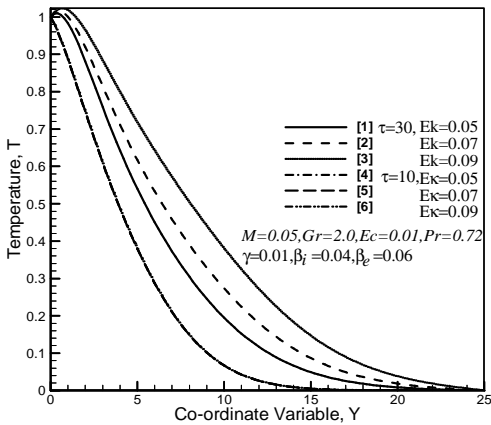


Figure 10: Temperature profiles for E_k

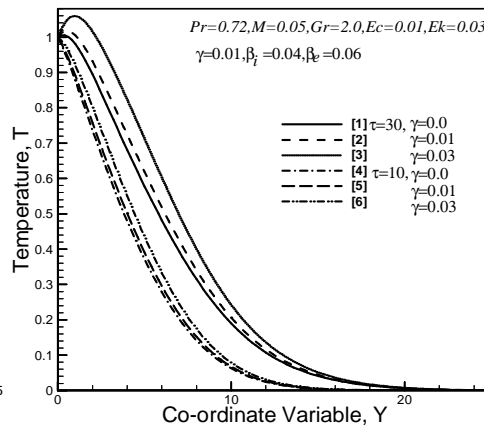


Figure 13: Temperature profiles for γ

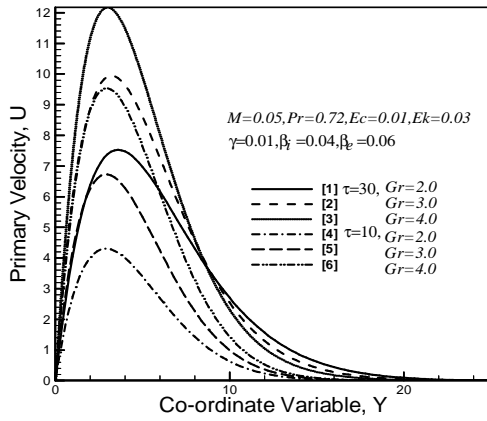


Figure 14: Primary velocity for G_r .

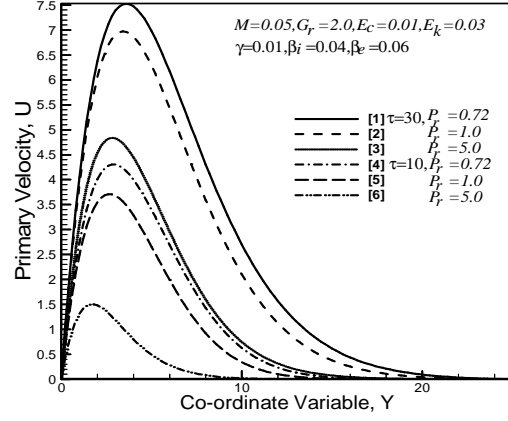


Figure 17: Primary velocity for P_r .

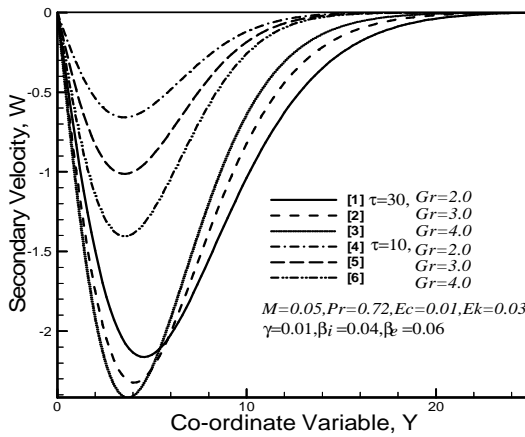


Figure 15: Secondary velocity for G_r .

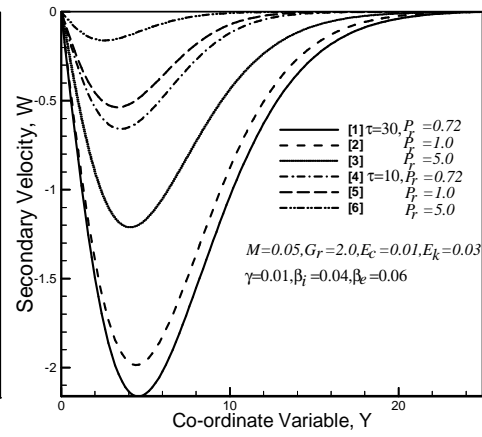


Figure 18: Secondary velocity for P_r .

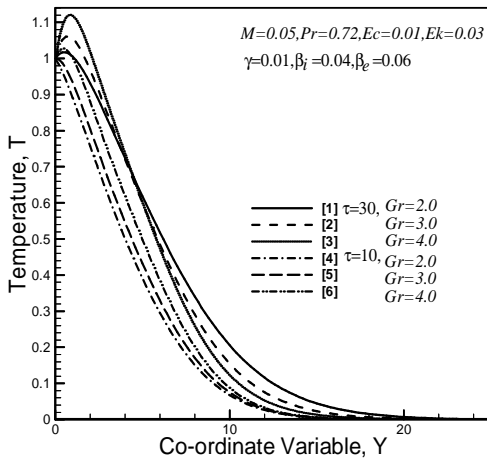


Figure 16: Temperature profiles for G_r .

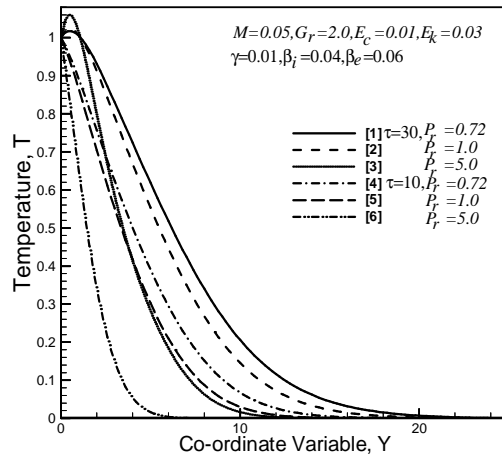


Figure 19: Temperature profiles for P_r .

Unsteady MHD-Free Convection Flow Past from a Rotating Vertical Plate

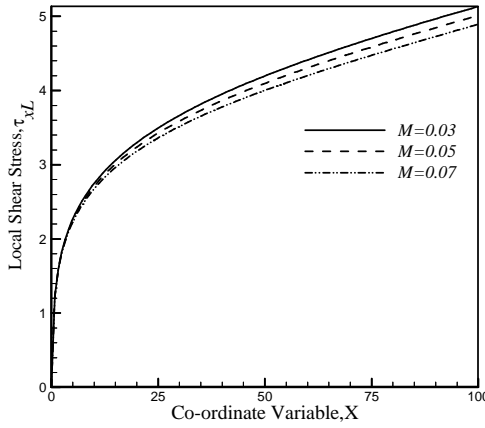


Figure 20: Effect of M on local shear stress in x – direction.

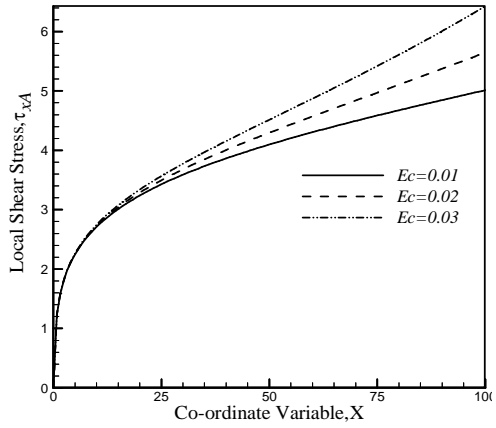


Figure 23: Effect of Ec on local shear stress in x – direction.

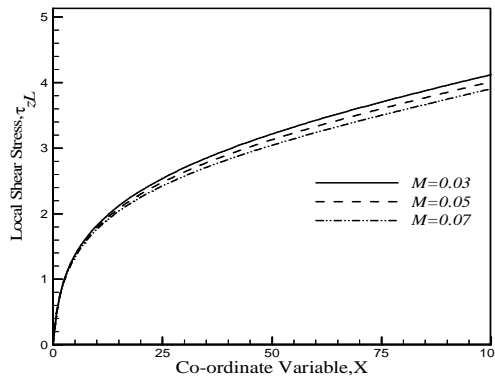


Figure 21: Effect of M on local shear stress in z – direction.

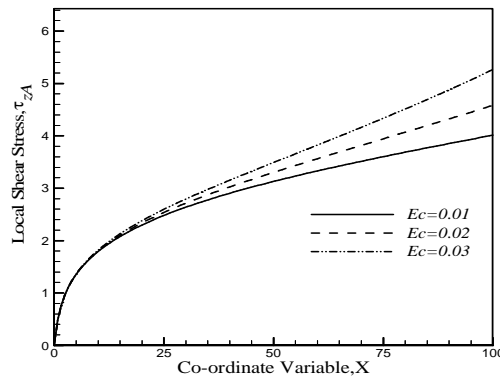


Figure 24: Effect of Ec on local Shear stress in z – direction.

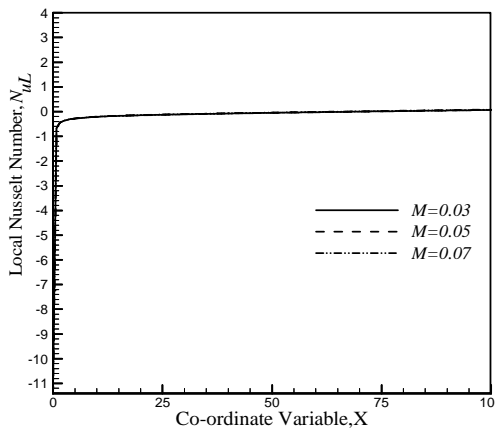


Figure 22: Effect of M on local nusselt number.

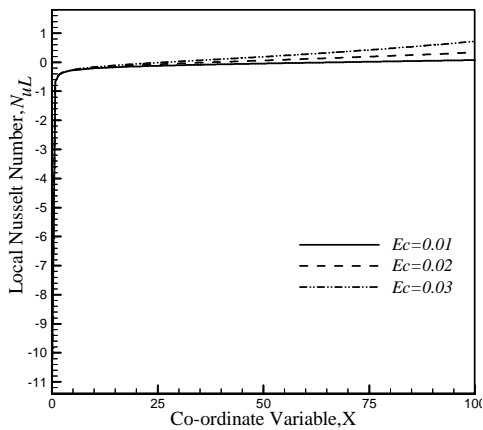


Figure 25: Effect of Ec on local nusselt number.

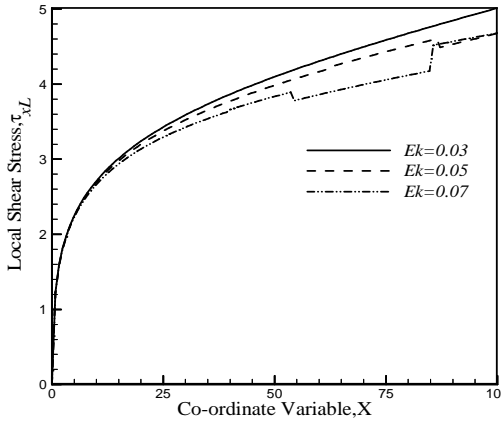


Figure 26: Effect of E_k on local shear stress in x – direction.

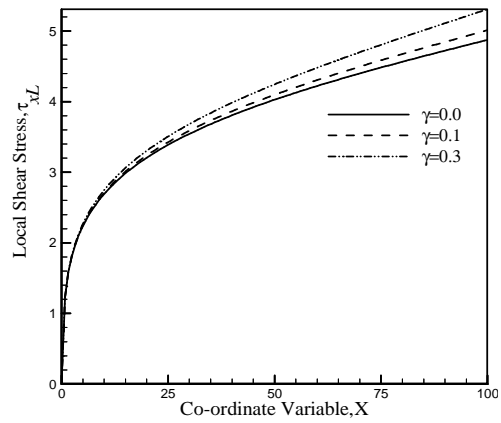


Figure 29: Effect of γ on local shear stress in x – direction.

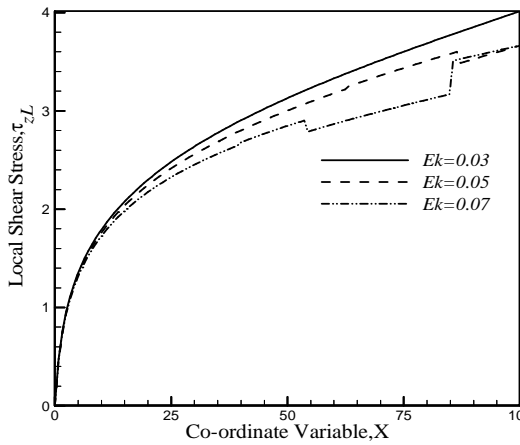


Figure 27: Effect of E_k on local shear stress in z – direction.

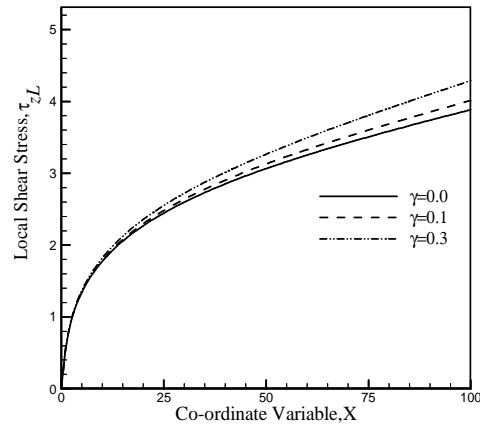


Figure 30: Effect of γ on local shear stress in z – direction.

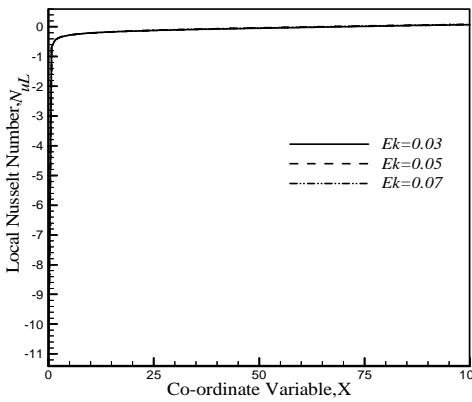


Figure 28: Effect of E_k on local nusselt number.

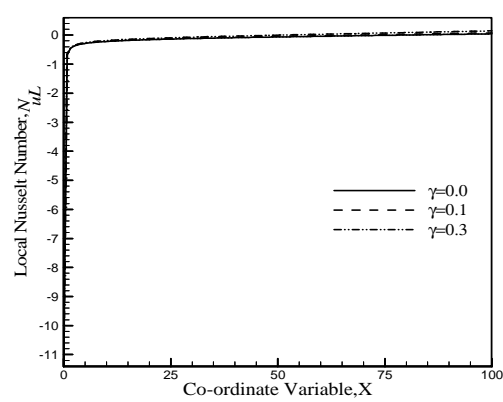


Figure 31: Effect of γ on local nusselt number.

Unsteady MHD-Free Convection Flow Past from a Rotating Vertical Plate

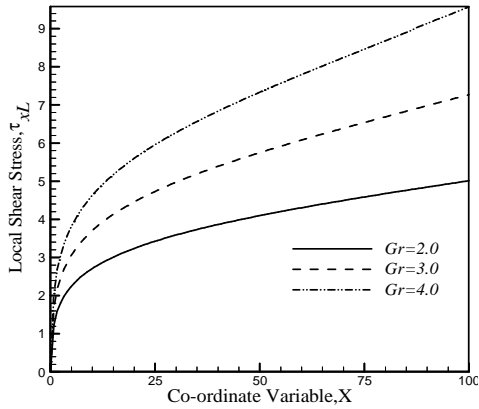


Figure 32: Effect of G_r on local shear stress in x – direction.

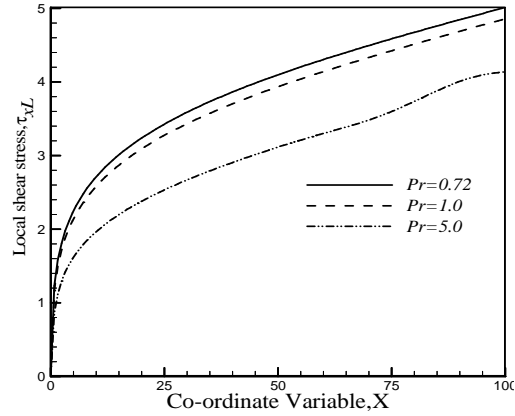


Figure 35: Effect of P_r on local shear stress in x – direction.

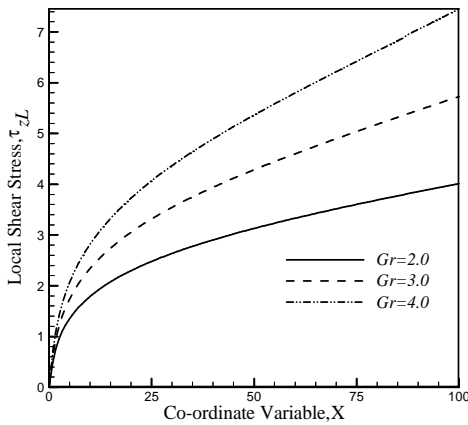


Figure 33: Effect of G_r on local shear stress in z – direction.

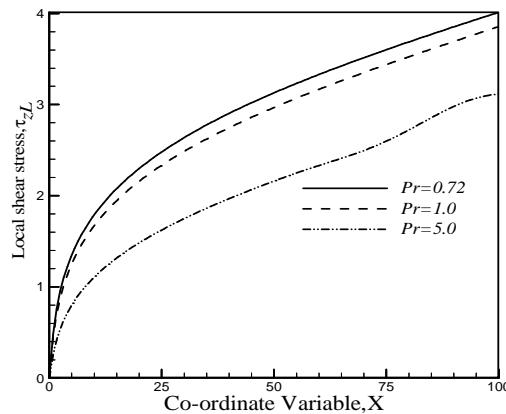


Figure 36: Effect of P_r on local shear stress in z – direction.

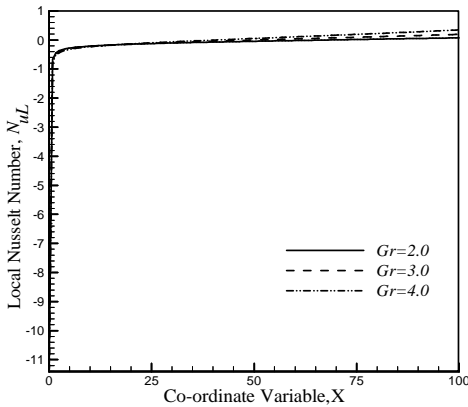


Figure 34: Effect of G_r on local nusselt number.

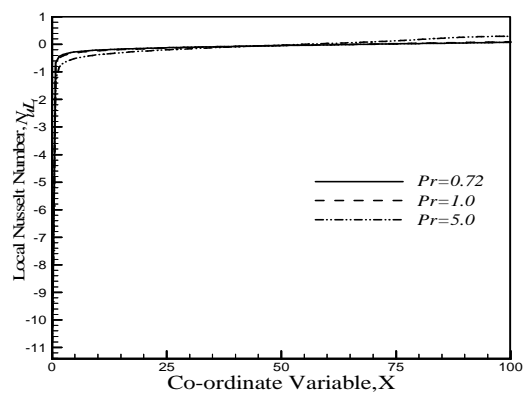


Figure 37: Effect of P_r on local nusselt number.

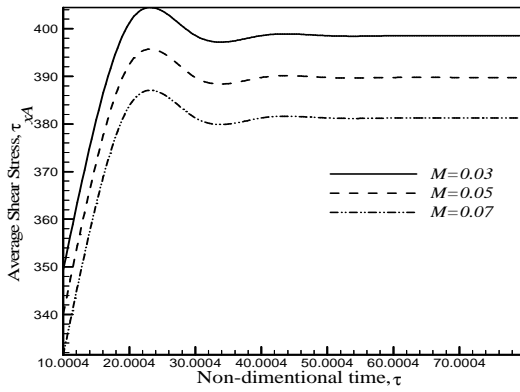


Figure 38: Effect of M on average shear stress in x – direction.

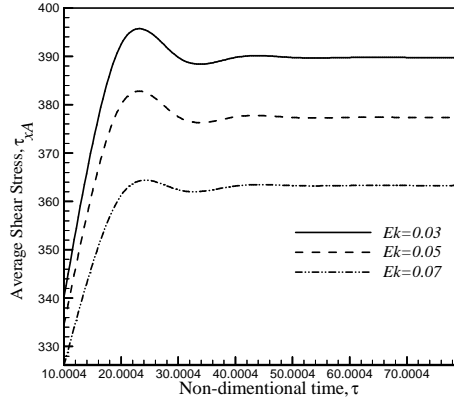


Figure 41: Effect of E_k on average shear stress in x – direction.

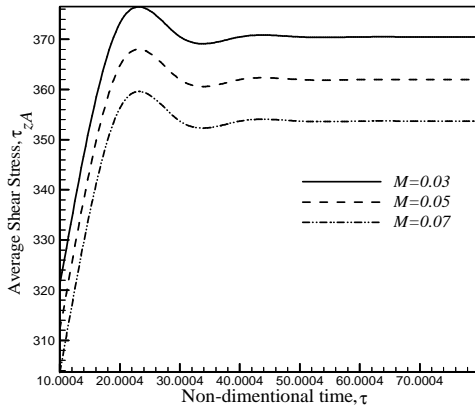


Figure 39: Effect of M on average shear stress in z – direction.

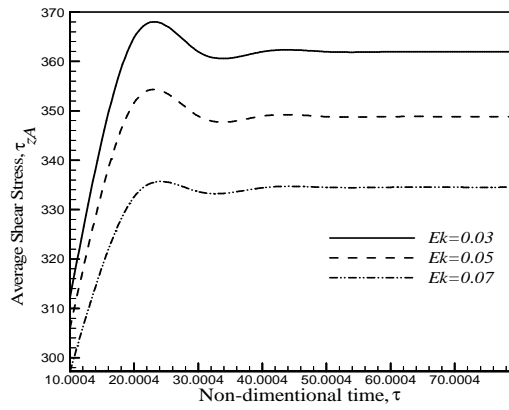


Figure 42: Effect of E_k on average shear stress in z – direction.

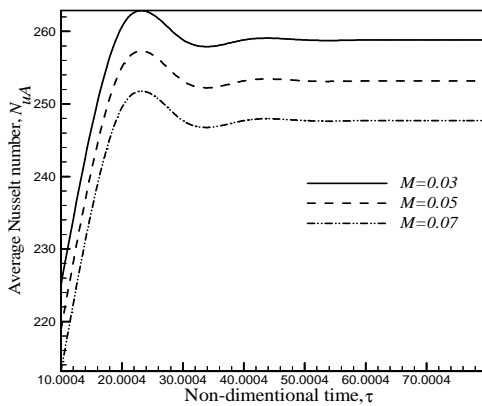


Figure 40: Effect of M on average nusselt number.

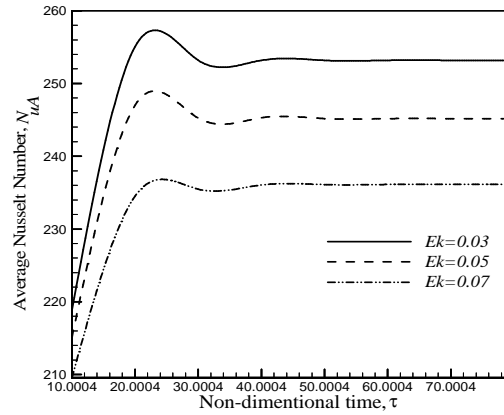


Figure 43: Effect of E_k on average nusselt number.

Unsteady MHD-Free Convection Flow Past from a Rotating Vertical Plate

in x -direction, average Shear Stress (τ_{AL}) in z -direction and average Nusselt number (N_{uA}) are plotted for different values of Ekman number (M) where $P_r = 0.72$, $G_r = 2.0$, $E_c = 0.01$, $M = 0.05$, $\beta_i = 0.04$, $\beta_e = 0.06$ and $\gamma = 0.01$. It has found that Steady-state average Shear Stress (τ_{xA}) in x -direction, average Shear Stress (τ_{AL}) in z -direction and average Nusselt number (N_{uA}) decrease for increasing of Ekman number (E_k).

6. Conclusion

The important findings of the investigation from graphical representation are listed below:

1. The primary velocity decreases with the increases of M , E_k , G_r and P_r while the secondary velocity increases with the increase of M , G_r , P_r , E_c and β_i .
2. The secondary velocity decreases with the increases of E_k and γ while the primary velocity increases with the increase of γ and E_c .
3. The temperature profiles increases with the increase of M , E_c , E_k and γ while it decreases with the increase of P_r and G_r .

REFERENCES

1. L.Debnath, S.C.Roy and A.K.Chatterjee, Effects of hall current on unsteady hydro-magnetic flow past a porous plate in a rotating fluid system, *Journal of Applied Mathematics and Mechanics (Zeitschrift für Angewandte Mathematik und Mechanik, ZAMM)*, 59 (1979) 469.
2. A.A.Raptis and C.P.Perdikis, Effects of mass transfer and free-convection currents on the flow past an infinite porous plate in a rotating fluid, *Astrophysics and Space Science*, 84(2) (1982) 457-461.
3. J.Hartmann and F.Lazarus, The influence of a transverse uniform magnetic field on the flow of a conducting fluid between two infinite parallel, stationary and insulated plates, *Danske Videnskab Selskab, Mat.-fys. Medd*, 15 (1937) 346-369.
4. M.A.Sattar and M.M.Alam, Unsteady hydromagnetic free convection flow with hall current and mass transfer along an accelerated porous plate with time dependent temperature and concentration, *Can. J. Phys.*, 70 (1992) 369
5. M.S.Islam, M.Samsuzzoha, S.Ara and P.Dey, MHD free convection and mass transfer flow with heat generation through an inclined plate, *Annals of Pure and Applied Mathematics*, 3(2) (2013) 129-141.
6. M.A.Rahman, M.A.Alim and M.J.Islam, Thermophoresis effect on MHD forced convection on a fluid over a continuous linear stretching sheet in presence of heat generation and power-law wall temperature, *Annals of Pure and Applied Mathematics*, 4(2) (2013) 192-204.

M. Wahiduzzaman, G.C.Mazumder, Md. Tajul Islam, A.Sarker and M.S.Uddin

7. M.Hasanuzzaman, B.Mandal and M.M.T.Hossain, A study of similarity solution of unsteady combined free and force convective laminar boundary layer flow about a vertical porous surface with suction and blowing, *Annals of Pure and Applied Mathematics*, 6(1) (2014) 85-97.
8. E.M.Abo-Eldahab and M.A.Aziz, Viscous dissipation and joule heating effects on MHD-free convection from a vertical plate with power-law variation in surface temperature in the presence of hall and ion-slip currents, *Applied Mathematical Modeling*. 29 (2005) 579-595.